Contract #FA9550-07-C-0033

FINAL REPORT. COMPUTATIONAL PREDICTION OF KINETIC RATE CONSTANTS

Period 1 February 2007 – 31 January 2009

Mark Ponton, ACES QC, LLC
Rodney J. Bartlett, University of Florida
ACES QC, LLC
1421 NW 47th Terrace
Gainesville, FL 32605
bartlett@qtp.ufl.edu
352-377-8257

The determination of gas phase thermal rate constants for chemical reactions even at ambient conditions is one of the most basic problems in chemistry. Thermal rate constants as a function of temperature are the critical component of all atmospheric[1] and combustion models [2-4]. They are also essential to understanding the initial steps in detonation. The enormous number of potential reactions---and dearth of experimental data for most of them--- emphasize the critical necessity of developing procedures that can *reliably* provide *a priori* rate constants [5-7]to complement experiment, and to help to fill in the gaps in the absence of experiment. Despite the enormous successes of quantum mechanical descriptions of the electrons in molecules-- i.e. electronic structure theory-- where several program systems exist like GAUSSIAN, ACES II [8], MOLPRO , TURBOMOLE, QCHEM, GAMESS, JAGUAR, MOPAC, HYPERCHEM [9], etc, that are extensively used to determine the structure, spectra, and energetics of molecules-- the equally basic, *kinetic* aspect of chemistry has not been as developed. Although programs and program suites like POLYRATE [10], CHEMRATE [11], VariFlex [12], UNIRATE [13], and MultiWell [14,15] exist for kinetics calculations, all of them require results from the electronic structure theory for input information.

As we have pointed out in our proposal entitled "Computational Prediction of Kinetic Rate Constants", there is a great need for electronic structure methods that are seamlessly tied to other programs that permit rate constant evaluation, or better, have accurate rate constant evaluation as an integral part of the suite of electronic structure programs, so that rate constants can be evaluated at virtually any applicable level of theory by non-expert users. In addition to ease of application, further attention has to be paid to improving the electronic structure theory that enables it to provide the highly accurate information specific to rate constants, that their reliable evaluation demands; and to the degree warranted, improve the procedures for the rate *constant evaluation itself.*

However, the challenges of *a priori* rate constant predictions are many:

(1) For PES with intrinsic barriers, kinetic theory begins with transition state (TS) information, defined as a saddle point on a reaction path of a temperature independent PES. Unlike molecules at normal bond lengths and angles, TS's are characterized by beginning to break and form bonds, so the electronic structure theory description is more demanding in terms of accuracy, and in terms of the

REPORT DOCUMENTATION PAGE

Form Approved
OMB No. 0704-0188

1. REPORT DATE *(DD-MM-YYYY)*	2. REPORT TYPE	3. DATES COVERED *(From - To)*
15-02-2009	Final Report	1 February 2007 - 31 January 2009

4. TITLE AND SUBTITLE
Phase 2. Final Report. Computational Prediction of Kinetic Rate Constants

5a. CONTRACT NUMBER
FA9550-07-C-0033

5b. GRANT NUMBER

5c. PROGRAM ELEMENT NUMBER

6. AUTHOR(S)
Mark Ponton, ACES QC, LC
Rodney Bartlett, University of Florida

5d. PROJECT NUMBER

5e. TASK NUMBER

5f. WORK UNIT NUMBER

7. PERFORMING ORGANIZATION NAME(S) AND ADDRESS(ES)
ACES QC, LC
1421 NW 47th Terrace
Gainesville, FL 32605-4564

8. PERFORMING ORGANIZATION REPORT NUMBER
AFSTTRII 08

9. SPONSORING/MONITORING AGENCY NAME(S) AND ADDRESS(ES)
AFOSR/PKC
875 North Randolph Street
Arlington, VA 22203

10. SPONSOR/MONITOR'S ACRONYM(S)

11. SPONSORING/MONITORING AGENCY REPORT NUMBER

12. DISTRIBUTION AVAILABILITY STATEMENT
Unlimited

13. SUPPLEMENTARY NOTES

14. ABSTRACT
The objective of this STTR has been to develop tools to make the evaluation of rate constants for gas phase reactions routine for many modest sized molecules. Such quantities are critical input to atmospheric and combustion models. They also provide critical information to designing procedures to destroy stock piles of nerve agents, and other waste products. However, it is often very difficult to experimentally measure such rate constants, making 'predictive' quantum chemistry often the best route to their determination. Unlike experiment, rate constants can also be computed under severe conditions including very high temperatures. The theoretical determination requires two steps: the application of electronic structure methods to determine geometries like that of transition states and and their associated energetics, such as activation barriers. Once this is done, then for most thermal rate constants reasonable values can be obtained from transition state theory (TST), variational transition state theory (VTST), RRKM, and related methods. The latter constitutes the dynamics portion of the effort, but the computationally determining step is the quantum mechanical calculations for the electronic structure. Most of the accuracy of the resultant rate constant also derives from that part of the calculation. Depending upon the size of molecule, there is a transition from simpler to more sophisticated methods.This project has introduced HF-DFT as the simplest possible method for their determination, since only a HF calculation followed by a 'tack-on' DFT estmate of correlation is required. At the other end we introduced lambdaCCSD(T) as the most sophisticated. In between standard DFT methods, MBPT2, CCSD, and CCSD(T) constitute a paradigm of methods of increasing sophistication. All of these are written into ACES II along with the TS methods for routine application. There is also an interface to POLYRATE to further exploit the ACES II input to that package for rate constant calculation. Several user friendly tools were added to ACES II to make such rate constant applications easier.

INSTRUCTIONS FOR COMPLETING SF 298

15. SUBJECT TERMS STTR Phase II Final Report					
16. SECURITY CLASSIFICATION OF:			17. LIMITATION OF ABSTRACT UU	18. NUMBER OF PAGES 25	19a. NAME OF RESPONSIBLE PERSON Rodney J. Bartlett
a. REPORT U	b. ABSTRACT U	c. THIS PAGE U			19b. TELEPONE NUMBER (*Include area code*) 352-392-6974

tools (analytical force calculations and reaction path following) needed to locate the TS's on the PES.

(2) For PES without intrinsic barriers, such as will occur with recombination reactions involving two radicals; rather than the energy path above, it is necessary to find the maximum of the free energy path, $\Delta G(T)$, to obtain rate constants To include the T dependence the appropriate partition functions have to be obtained along the path, which requires vibrational frequency information at every point.

(3) The dynamics part of the problem required to evaluate the rate constants once the electronic structure problem has been solved, must be reliable itself. The current choices for this step are transition-state theory (TST), RRKM, variational (VTST), semi-classical generalizations of Miller's flux-flux auto correlation function approach (SCFFAF),[16,17] classical trajectories, and maybe some other models based upon updated collision theory concepts. The accuracy of the results obtained will depend greatly upon both the rate evaluation and the accuracy of the electronic structure results.

(4) Thermal rate constants are of many types and they can be affected by tunneling when light atoms are involved, van der Waals' minima on the PES[18], multiple reaction channels (transition states), and non-adiabatic effects with multiple PESs. Tunneling, in particular, is usually treated as an 'add-on' to VTST with various small and large curvature tunneling corrections possible. The FFAF approach[17] begins to put tunneling in more satisfactorily, but, in practice, only within a semi-classical approximation when this tool has been used for multi- atom systems.[16]

So unlike most applications of electronic structure theory, the wealth of different types of reactions, different conditions, and the more global PES information required, makes it extremely difficult to develop a few, general-purpose procedures that can be refined until accurate rate constants are obtained from something approximating a 'point and click' computational chemistry calculation.

During the three years covered by the proposal "Computational Prediction of Kinetic Rate Constants" awarded to the ACES QC and the University of Florida sponsored by the United States Air Force Office of Scientific Research (AFOSR) through a Phase II STTR, as mandated, we have primarily focused on the electronic structure development component and continued developing in house rate program (ACESRATE) and the interface software to other well established rate programs which we started during the phase I stage. The latter developments are essential in order to make the electronic structure data easily available to the kinetic programs. Before proceeding to discuss them in detail, in summary our accomplishments include the following:

- Development, implementation and calibration of two new electronic structure methods (HF-DFT and ΛCCSD(T)).

- Upgrading KS-DFT implementation, adding the KS-DF gradients and improving the stationary state search algorithms in ACES II and in ACES III

- Developing the ACESRATE program suite in-house and starting to develop interfaces to vender supplied rate programs such as POLYRATE and VENUS.

- Three articles in peer reviewed journals have been published already and several more are in preparation.

Electronic Structure Method Development

ΛCCSD(T) Energies and gradients:

The gold standard of quantum chemistry is CCSD(T)[19] because of its high accuracy near equilibrium and reasonable computational cost. Unfortunately, as illustrated in Fig. 1 below, the method fails

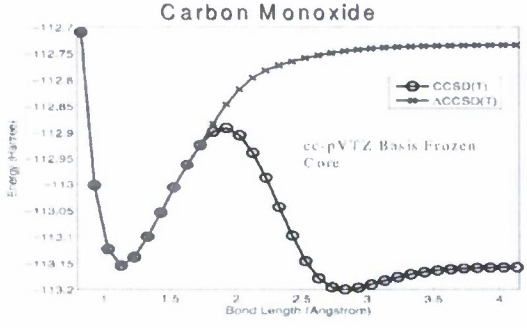

dramatically away from equilibrium (using a spin-restricted reference) and has the incorrect bond-breaking slope with an unrestricted reference. The breakdown of CCSD(T) can be traced to its dependence on CCSD amplitudes. For a bond-breaking situation, the CCSD wavefunction is qualitatively wrong; however, the energy is only a linear function of the amplitudes and is well behaved. CCSD(T) is a quadratic function of the CCSD amplitudes leading to a qualitatively incorrect energy.

By applying similarity-transformed perturbation theory to the CCSD stationary energy functional, one can show that the leading order correction is linear in the T amplitudes,

and is also linear in the Λ amplitudes from CCSD gradient theory. This correction is called the ΛCCSD(T) method:

$$E_{\Lambda\mathrm{CCSD(T)}} = \langle 0|(1+\Lambda)\overline{H}|0\rangle + \left(\frac{1}{3!}\right)^2 \langle 0|\Lambda H^{(1)}\Big|_{ijk}^{abc}\rangle \frac{1}{\varepsilon_{ijk}^{abc}} \langle {}_{ijk}^{abc}\Big|\left(H^{(1)}T_2\right)_C|0\rangle$$

The Λ amplitudes are qualitatively well behaved, and that substantially improves bond-breaking behavior for the perturbation correction. Only twice as expensive as CCSD(T), ΛCCSD(T)[20] represents the simplest extension (both theoretically and computationally) to CCSD(T) that improves bond breaking, and gives results of the same quality as the more complicated and formally less satisfactory CR-CCSD(T)$_L$ and CCSD(2)$_T$ methods. The latter are either not size-extensive, the rationale for all coupled-cluster methods, or fail to be invariant to orbital rotations.

For the identification of stationary points, it is necessary to not only have energies, but also analytical derivatives. For a perturbative method like ΛCCSD(T) this is not trivial; to be able to apply the generalized Hellman-Feynman theorem, a stationary formulation of ΛCCSD(T) needed to be developed. Then the derivative is defined by,

$$\frac{\partial E_{\Lambda\mathrm{CCSD(T)}}}{\partial\chi} = \langle 0|(1+\Lambda+\Pi)\overline{H}^{\chi}|0\rangle + \langle 0|(1+\Lambda)\left(\overline{H}^{\chi}\Sigma\right)_C|0\rangle + \langle 0|\Lambda H^{(1),\chi}T_3^{[2]}|0\rangle$$
$$+\langle 0|\Lambda_3^{[2]}H^{(0),\chi}T_3^{[2]}|0\rangle + \langle 0|\Lambda_3^{[2]}\left(H^{(1),\chi}T_2\right)_C|0\rangle$$

We have now implemented ΛCCSD(T) and its analytical derivatives to make such applications routinely possible for transition states. Having correct potential energy surfaces for the entire range; from equilibrium to bond breaking, is an essential component of the rate constant calculations. We found that despite the substantially increased improvement in bond breaking, for the determination of stationary points, including transition states, CCSD(T) and ΛCCSD(T) performed virtually identically[21,22]. The transition state structure of the nitromethane–methylnitrite rearrangement (in Table 1) and the reaction path (Fig. 2) computed at CCSD(T) and ΛCCSD(T) support this conclusion. Another system that we studied is the concerted bond breaking of RDX. It is shown that similar to nitromethane–methylnitrite rearrangement, both the CCSD(T) and ΛCCSD(T) show essentially the same characteristics. As shown in Table 2, the same conclusion is reached for the barrier heights of the series of reactions from a selection compiled by Truhlar *et al.*[23] for the purpose of benchmarking electronic structure methods for rate constant calculations.

Table 1: Nitromethane to methylnitrite optimized transition state results for B3LYP, CCSD(T) and ΛCCSD(T). Energies are zero-point corrected.

Parameter	B3LYP	CCSD(T)	ΛCCSD(T)
Barrier Height (kcal/mol)			
$\Delta E_f^{\ddagger}$	64	67.24	67.47
$\Delta E_r^{\ddagger}$	66	69.53	69.88
Bond Lengths (Å)			
CN	1.964	1.895	1.891
CO(1)	1.999	1.970	1.969
O(1)N	1.298	1.323	1.321
O(2)N	1.198	1.206	1.206
Bond Angles (°)			
O(1)NC	73.0	73.1	73.2
O(1)NO(2)	*	118.8	118.9

* Angle unavailable.

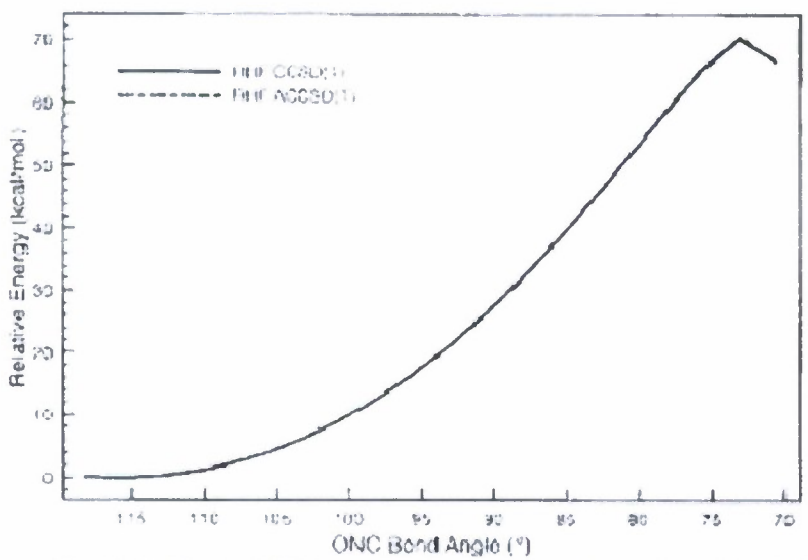

Fig 2. NMT to MNT reaction path computed by CCSD(T) and ΛCCSD(T).

Table 2: Barrier Heights for well-characterized reactions from Minnesota data set. Energies and errors from best experimental estimates are in kcal/mol.

Reaction		Barrier Height		Error from Best Estimate	
		CCSD(T)	ACCSD(T)	CCSD(T)	ACCSD(T)
$H+N_2O \rightarrow OH+N_2$	$V_f^{\ddagger}$	18.80	19.01	0.66	0.90
	$V_r^{\ddagger}$	83.73	84.24	0.51	1.02
$H+FH \rightarrow HF+H$	$V_f^{\ddagger}$	13.57	13.63	1.39	1.45
	$V_r^{\ddagger}$	13.57	13.63	1.39	1.45
$H+OH \rightarrow HOH$	$V_f^{\ddagger}$	19.63	19.73	1.63	1.73
	$V_r^{\ddagger}$	19.63	19.73	1.63	1.73
$H+FCH_3 \rightarrow HF+CH_3$	$V_f^{\ddagger}$	31.92	31.98	1.51	1.60
	$V_r^{\ddagger}$	57.69	57.71	0.67	0.72
$H+F_2 \rightarrow HF+F$	$V_f^{\ddagger}$	2.3.	2.63	0.10	0.36
	$V_r^{\ddagger}$	105.96	106.03	-0.22	0.15
$CH_3+FCl \rightarrow CH_3F+Cl$	$V_f^{\ddagger}$	6.10	6.82	-0.97	-0.61
	$V_r^{\ddagger}$	61.81	62.35	1.61	2.18
$F^- + CH_3F \rightarrow FCH_3+F^-$	$V_f^{\ddagger}$	-1.29	-1.28	-0.96	-0.94
	$V_r^{\ddagger}$	-1.29	-1.28	-0.96	-0.94
$F^- \cdots CH_3F \rightarrow FCH_3 \cdots F^-$	$V_f^{\ddagger}$	13.35	13.34	-0.03	-0.04
	$V_r^{\ddagger}$	13.35	13.34	-0.03	-0.04
$Cl^- + CH_3Cl \rightarrow ClCH_3 + Cl^-$	$V_f^{\ddagger}$	2.37	2.52	-0.73	-0.58
	$V_r^{\ddagger}$	2.37	2.52	-0.73	-0.58
$Cl^- \cdots CH_3Cl \rightarrow ClCH_3 \cdots Cl^-$	$V_f^{\ddagger}$	13.03	13.15	-0.58	-0.46
	$V_r^{\ddagger}$	13.03	13.15	-0.58	-0.46
$F^- + CH_3Cl \rightarrow FCH_3 + Cl^-$	$V_f^{\ddagger}$	-11.50	-11.41	-1.96	-1.87
	$V_r^{\ddagger}$	22.28	22.29	2.17	2.18
$F^- \cdots CH_3Cl \rightarrow FCH_3 \cdots Cl^-$	$V_f^{\ddagger}$	2.30	2.36	-0.59	-0.53
	$V_r^{\ddagger}$	31.70	31.09	2.05	2.07
$OH^- + CH_3F \rightarrow HOCH_3 + F^-$	$V_f^{\ddagger}$	-3.89	-3.84	-1.11	-1.06
	$V_r^{\ddagger}$	16.23	16.31	-1.10	-1.02
$OH^- \cdots CH_3F \rightarrow HOCH_3 \cdots F^-$	$V_f^{\ddagger}$	10.67	10.71	-0.29	-0.25
	$V_r^{\ddagger}$	17.86	17.85	0.86	0.65
$H+CO \rightarrow HCO$	$V_f^{\ddagger}$	1.07	1.13	0.90	0.96
	$V_r^{\ddagger}$	24.90	22.07	-0.09	-0.01
$H+C_2H_4 \rightarrow CH_3CH_2$	$V_f^{\ddagger}$	2.68	2.75	0.96	1.03
	$V_r^{\ddagger}$	11.75	11.96	0.00	0.21
$CH_3+C_2H_4 \rightarrow CH_3CH_2CH_2$	$V_f^{\ddagger}$	6.92	7.13	0.07	0.28
	$V_r^{\ddagger}$	32.60	32.18	-0.47	-0.19
$HCN \rightarrow HNC$	$V_f^{\ddagger}$	18.47	18.52	0.31	0.37
	$V_r^{\ddagger}$	33.50	33.09	0.45	0.58
Average Absolute Error				0.85	0.89

Non Variational Density Functional Theory (HF-DFT) Energies and Gradients:

The non variational DFT (HF-DFT)[24] methods do not involve solving Kohn-Sham equations. They are designed to replace the HF exact exchange energy by the energy of a chosen exchange-correlation functional computed with the HF density. The assumption is that by choosing an exchange correlation functional instead of the HF exchange, the HF energy is improved by the correlation effects introduced by the exchange correlation functional. The HF-DFT energy and gradient expressions are straightforward extensions the HF energy and gradient expressions. For example, the energy and the gradient designated as E^{HF-DFT} and $\frac{dE^{HF-DFT}}{dR_x}$ can be written as

$$E^{HF-DFT} = E_{Nuclear-Nuclear} + E_{Kinetic}\left(\varphi^{Hartree-Fock}\right) + E_{Nuclear-Electron}\left(\varphi^{Hartree-Fock}\right) +$$

$$E_{Coulomb-Electron-Electron}(\varphi^{Hartree-Fock}) + E^{Becke-LYP}_{Exchange-correlation}\left(\rho^{Hartree-Fock}, \nabla\rho^{Hartree-Fock}\right)$$

$$\frac{dE^{HF-DFT}}{dR_x} = \sum_{\sigma}\sum_{\mu\nu} F_{\mu\nu}^{KS-\sigma} \left.\frac{\partial P_{\mu\nu}^{\sigma}}{\partial R_x}\right|_{\mu,\nu} + \left.\frac{\partial E^{HF-DFT}}{\partial R_x}\right|_{P}$$

Where the density matrix $P_{\mu\nu}^{\sigma} = \sum_{i\in OCC} C_{\mu i}^{\sigma} C_{\nu i}^{\sigma}$ and the KS-Fock operator (for the gradients) is given by

$$F_{\mu\nu}^{KS-\sigma} = \left(\mu\left|-\frac{1}{2}\nabla^2 - \sum_{A}^{M}\frac{Z_A}{r_{A1}}\right|\nu\right) + \sum_{\lambda\delta} P_{\lambda\delta}(\mu\nu\,|\,\lambda\delta) + V_{xc}^{Becke-LYP}$$

When expanded the HF-DFT energy gradient expression

$$\frac{dE}{dx} = \sum_{\mu\nu} P_{\mu\nu} h_{\mu\nu}^{x} + \frac{1}{2}\sum_{\mu\nu\lambda\sigma} P_{\mu\nu} P_{\lambda\sigma} (\mu\nu\,|\,\lambda\sigma)^{x} + E_{xc}^{x}(P^{\alpha}, P^{\beta})$$

$$- \sum_{\sigma}\sum_{i}\sum_{j} S_{ij,\sigma}^{x} F_{ij,\sigma} + 2\sum_{\sigma}\sum_{i}\sum_{a} U_{ia,\sigma}^{x} F_{ia,\sigma}$$

Where $E_{xc} = \int f(\rho_{\alpha}, \rho_{\beta}, ...)dr \quad E_{xc} = \sum_{A}\sum_{i} w_{Ai} f(\rho_i^{\alpha}, ..., \vec{r}_{Ai})$

$$\nabla_B E_{xc} = \sum_{A}\sum_{i} [w_{Ai}\nabla_B f(\rho_i^{\alpha}, ..., \vec{r}_{Ai}) + \nabla_B w_{Ai} f(\rho_i^{\alpha}, ..., \vec{r}_{Ai})]$$

For the most part, the cost involving adding the exchange correlation energy is small and one can safely assume that there is no additional cost beyond the cost of obtaining the HF solutions, but the energies are corrected for correlation. Furthermore, since it depends upon a HF solution to get the density, there is no self-interaction failure, but all correlation effects are assumed to come solely from the evaluation of the LYP functional, in a non-self-consistent manner. The results for a large number of molecules have been surprisingly accurate, as the mean absolute errors (MAE) compare favorably to those from the very high-level CCSD(T) method. For example for equilibrium geometries, the average absolute error for a large number of small molecules compared to experiment is 0.005 Angstroms for bond lengths, the same as CCSD(T), 1.7 degrees for the bond angle, compared to 1.9 for CCSD(T), 40 cm^{-1} error in vibrational frequencies, compared to 30 cm^{-1} for the latter, and does better for atomization energies, 3.6 kcal/mol compared to 11.5 kcal/mol[24].

The primary data that are of interest for rate constant calculation are activation energies, structures, and vibrational frequencies of stationary points (and in some cases at points in the vicinity of a transition state). Until this work, the performance of HF-DFT for transition state structures, frequencies and activation barriers was not known. To facilitate such calibrations, we implemented the analytical gradients for HF-DFT[25]. In Table 3, we show the structures of the transition states of a series of reactions (18 altogether) obtained with HF-DFT along with the QCISD results from the literature obtained with the same MG3[26] basis sets. As shown in Table 4, the average absolute difference between the QCISD/MG3 and HF-DFT/MG3 results are 0.03 (Angstroms) and 2.6 (degrees) for bond lengths and angles respectively.

The accuracy of the activation energy is perhaps the most important factor that governs the accuracy of the thermal rate constants since the error in the rate constant grows exponentially with the error in the activation energy. In order to calibrate the accuracy of HF-DFT activation energies, we have done two sets of calculations. In one case, we have used the geometries optimized at the MG3/QCISD level available in the literature and the single point HF-DFT energies of reactants and transition states are computed. This set is comprised of 40 reactions as compiled by Truhlar and coworkers[23] in order to calibrate new DFT functionals. In the other set (a subset of reactions from the previous set) the activation energies are computed at the HF-DFT optimized transition state structures. For comparisons, we also show the HF and KS-DFT activation energies (also obtained at the TS geometry optimized at the HF and KS-DFT level). As shown in Table 5, the average absolute error (the best available values from the literature is chosen as the reference) of the HF-DFT activation energies is 2 kcal/mol. A 2 kcal/mol average error for HF-DFT is remarkable in the sense that there is practically no extra cost beyond the cost for HF calculation. That is, this is the simplest possible calculation that includes electron correlation, a necessity for activation barriers and transition states. We conclude that HF-DFT is a cost effective and sufficiently accurate method to be used in rate constant calculations.

Table 3: Comparisons of HF-DFT transition state structures with publish data (distances are in angstroms and angles are in degrees).

reaction	QCISD/MG3	HFDFT/MG3	error	Abs(error)
OH + H2 -> H + H2O				
tst(H--O...H--H)				
R(H--O)	0.967	0.978	-0.01	0.01
R(O...H)	1.3165	1.4121	-0.1	0.1
R(H--H)	0.833	0.805	0.03	0.03
A(H--O...H)	97.19	97.96	-0.77	0.77
A(O...H--H)	165.48	160.46	5.02	5.02
CH3 + H2 -> H + CH4				
tst(CH3....H--H)				
R(C...H)	1.382	1.431	-0.05	0.05
R(C--H1)	1.083	1.086	-0	0
R(H—H)	0.9040	0.8773	0.03	0.03
A(C..H--H)	180	180	0	0
A(C--H..H)	114.75	102.49	12.3	12.3
OH + CH4 -> CH3 + H2O				
tst(CH4..O--H)				
R(O--H)	0.966	0.977	-0.01	0.01
R(H...O)	1.227	1.396	-0.17	0.17

R(C--H)	1.084	1.088	-0	0
A(C--H..O)	173.68	174.08	-0.4	0.4
A(H....O--H)	97.7	97.38	0.32	0.32
A(H...C--H)	104.25	104.65	-0.4	0.4
A(H--C-H)	112.99	112.33	0.66	0.66
H + CH3OH -> CH2OH + H2				
tst(HOCH3..H)				
R(c--O)	1.384	1.396	-0.01	0.01
R(O--H)	0.957	0.967	-0.01	0.01
R(C--H)	1.089	1.095	-0.01	0.01
R(C--H)	1.084	1.089	-0.01	0.01
R(C...H)	1.315	1.294	0.02	0.02
R(H....H)	0.969	0.987	-0.02	0.02
A(C--O--H)	109.207	109.78	-0.57	0.57
A(O--C--H)	115.07	115.04	0.03	0.03
A(C....H..H)	177.479	178.16	-0.68	0.68
A(H-CH)	109.207	109.78	-0.57	0.57
A(H-CH)	109.819	109.58	0.24	0.24
A(H-CH)	110.068	110.65	-0.58	0.58
OH + NH3 - > H2O + NH2				
tst(NH3..OH)				
R(N--H)	1.016	1.020	-0	0
R(N--H)	1.016	1.020	-0	0
R(N--H)	1.153	1.100	0.05	0.05
R(H....O)	1.259	1.383	-0.12	0.12
R(H--O)	0.964	0.975	-0.01	0.01
A(H--N--H)	106.64	107.21	-0.56	0.56
A(H--N--H)	108.25	106.73	1.53	1.53
A(N--H--O)	150.42	148.05	2.37	2.37
A(H--O--H)	104.31	106.8	-2.48	2.48
F + H2 -> H + HF				
tst(H--H...F)				
R(H--H)	0.774	0.7707	0	0
R(H...F)	1.466	1.5886	-0.12	0.12
A(H--H...F)	152.06	108.16	43.9	43.9
H + PH3 -> PH2 + H2				
tst(PH2--H...H)				

R(P--H)	1.4139	1.424	-0.01	0.01
R(P--H)	1.414	1.424	-0.01	0.01
R(P-..H)	1.484	1.46	0.02	0.02
R(H....H)	1.264	1.475	-0.21	0.21
A(H--P--H)	93.49	92.908	0.59	0.59
A(H--P-..H)	92.57	92.397	0.17	0.17
A(P-..H..H)	166.75	171.12	-4.37	4.37
H + ClH' -> HCl + H				
tst(H--Cl....H)				
R(H--Cl)	1.485	1.477	0.01	0.01
R(Cl...H)	1.485	1.478	0.01	0.01
A(H--Cl...H)	180	180	0	0
OH + H -> H2 + O				
tst(O--H...H)				
R(O--H)	1.189	1.3128	-0.12	0.12
R(H...H)	0.911	0.8358	0.08	0.08
A(O--H...H)	180	180	0	0
H + trans-N2H2 -> H2 + N2H				
tst(HNN--H...H)				
R(N--N)	1.225	1.2582	-0.03	0.03
R(H--N)	1.030	1.0185	0.01	0.01
R(N-..H)	1.117	1.0619	0.06	0.06
R(H--H)	1.179	1.3798	-0.2	0.2
A(H--N--N)	107.41	121.81	-14.4	14.4
A(N--H--H)	170.55	169.49	1.07	1.07
A(N--N-..H)	107.04	119.43	-12.4	12.4
H + H2S -> H2 + HS				
tst(HS-..H...H)				
R(H--S)	1.337	1.3487	-0.01	0.01
R(S-..H)	1.429	1.3965	0.03	0.03
R(H...H)	1.149	1.332	-0.18	0.18
A(H--S-..H)	91.152	91.884	-0.73	0.73
A(S-..H...H)	172.61	179.3	-6.68	6.68

O + HCl -> OH + Cl				
tst(O…H--Cl)				
R(O…H)	2.482	2.4829	0	0
R(H-…Cl)	1.414	1.4706	-0.06	0.06
A(O…H-..Cl)	22.43	19.435	3	3
CH4 + NH -> NH2 + CH3				
tst(H3C-…H..N-H)				
R(H--C)	1.083	1.0867	-0	0
R(C-..H)	1.3953	1.4002	-0	0
R(H…N)	1.2117	1.2059	0.01	0.01
R(N--H)	1.0315	1.0387	-0.01	0.01
A(H--C--H)	114.59	114.72	-0.12	0.12
A(H--C-..H)	101.54	114.72	-13.2	13.2
A(H…N--H)	174.46	176.36	-1.9	1.9
C2H6 + NH -> NH2 + C2H5				
tst(H3C-CH2-..H…N--H)				
R(H--C)	1.093	1.0987	-0.01	0.01
R(H--C)	1.090	1.094	-0	0
R(H--C)	1.089	1.094	-0	0
R(C--C)	1.508	1.5141	-0.01	0.01
R(C-H)	1.086	1.0912	-0	0
R(C-H)	1.086	1.0911	-0	0
R(C-..H)	1.372	1.337	0.04	0.04
R(H…N)	1.233	1.2639	-0.03	0.03
R(N--H)	1.032	1.0386	-0.01	0.01
A(H--C--H)	107.447	107.3	0.14	0.14
A(H--C--H)	107.451	107.86	-0.41	0.41
A(H--C..C)	111.006	107.86	3.15	3.15
A(C--C-H)	115.596	115.55	0.04	0.04
A(C--C-H)	115.75	115.54	0.21	0.21
A(C--C-..H)	106.615	105.78	0.84	0.84
A(C-..H..N)	175.085	178.57	-3.49	3.49
A(H…N-H)	94.92	99.646	-4.73	4.73
C2H6 + NH2 -> C2H5 + NH3				
tst(H3C-CH2-..H..NH2)				
R(H--C)	1.093	1.0975	-0	0

R(H--C)	1.089	1.0933	-0	0
R(H--C)	1.089	1.094	-0	0
R(C--C)	1.511	1.521	-0.01	0.01
R(C-H)	1.087	1.092	-0	0
R(C-H)	1.087	1.0919	-0	0
R(C-..H)	1.294	1.2496	0.04	0.04
R(H...N)	1.295	1.3661	-0.07	0.07
R(N--H)	1.021	1.0291	-0.01	0.01
R(N--H)	1.021	1.0286	-0.01	0.01
A(H--C--H)	107.75	107.52	0.23	0.23
A(H--C--H)	107.75	107.51	0.24	0.24
A(H--C..C)	111.11	111.31	-0.19	0.19
A(C--C-H)	114.80	114.34	0.47	0.47
A(C--C-H)	114.80	114.38	0.43	0.43
A(C--C-..H)	105.13	106.54	-1.41	1.41
A(C-..H..N)	176.80	176.66	-71.5	71.5
A(H...N-H)	99.3	99.066	0.23	0.23
A(H..N--H)	99.3	99.611	-0.31	0.31
NH2 + CH4 -> CH3 + NH3				
tst(H3C-..H...NH2)				
R(H--C)	1.0848	1.0889	-0	0
R(H--C)	1.0848	1.089	-0	0
R(H--C)	1.0841	1.0882	-0	0
R(C-..H)	1.3141	1.3162	-0	0
R(H...N)	1.2702	1.2762	-0.01	0.01
R(N--H)	1.0209	1.0286	-0.01	0.01
R(N--H)	1.0209	1.0286	-0.01	0.01
A(H-N-H)	113.29	112.89	0.41	0.41
A(H-N-H)	113.44	112.9	0.55	0.55
A(H-N-..H)	103.78	104.15	-0.37	0.37
A(C-..H...N)	172.15	172.19	-0.03	0.03
A(H...N--H)	99.831	100.2	-0.37	0.37
A(H..N--H)	99.833	100.19	-0.36	0.36
Cl + H2 -> HCl + H				
tst(Cl...H--H)[A]				
R(Cl...H)	1.5438	1.3615	0.18	0.18
R(H--H)	0.7740	1.1846	-0.41	0.41
A(Cl...H--H)	180	180	0	0

Cl + H2 -> HCl + H	QCISD	Best-QCISD	HFDFT	Best-HFDFT	QCISD-HFDFT	Best
tst(Cl...H—H)						
R(Cl...H)	1.543	-0.113	1.361	0.069	0.18	1.43
R(H--H)	0.774	0.207	1.184	-0.203	-0.41	0.981

*The worst example, presented first in Table 1, would appear to be Cl + H_2, but this is misleading. In this case the QCISD/MG3 'reference' structure is very poor. So actually, the error for HF-DFT compared to the best possible results is much better, attesting to HF-DFT's accuracy (the "best values" are taken from. *Phys. Chem.* A **2001**, 105, 2936-2941)

Table 4: The error analysis of HF-DFT bond lengths, angles and activation energies (the reference values are taken from *J. Phys. Chem. A*, Vol. 104, 4811, 2000). The distances, angles and energies are in angstroms, degrees and kcal/mol respectively.)

Error	(QCISD-HF-DFT)	ABS(QCISD-HFDFT)
Distance(angstroms)	-0.02	0.038
Angle(degree)	0.1	2.64

Errors	Best-HFDFT	Best-QCISD	HFDFT-QCISD
(method1-method2)	-0.12	-1.02	-2.13
Absolute(method1-method2)	2.28	2.47	3.17

Table 5: Comparison of the HF-DFT activation energies with the literature values. The HF-DFT activation energies are computed at the same geometry (QCISD/MG3) using the same basis set (MG3) and the literature data is complied by Truhlar and coworkers[23].

reactions	HF DFT/MG3//QCISD/MG3 kcal/mol	QCISD/MG3 // QCISD/MG3 kcal/mol	best activation energy kcal/mol	HF DFT-QCISD kcal/mol	HF DFT - Best value kcal/mol
Cl + H2 -> HCl + H	5.92	12.73	8.7	-6.81	-2.78
H+HCl --> Cl + H2	1.24	7.01	5.6	-5.77	-4.36
OH + H2 -> H + H2O	4.91	7.77	5.7	-2.86	-0.79
H+H2O -> OH + H2	18.42	21.2	22	-2.78	-3.58
CH3 + H2 -> H + CH4	10.64	13.82	12.1	-3.18	-1.46
CH4 + H -> CH3 + H2	10.97	15.75	15	-4.78	-4.03
OH + CH4 -> CH3 + H2O	5.87	9.34	6.7	-3.47	-0.83
H2O + CH3 -> OH + CH4	19.06	20.84	20.2	-1.78	-1.14
H + CH3OH -> CH2OH + H2	5.58	10.96	7.3	-5.38	-1.72
H2 + CH2OH -> H + CH3OH	14.63	17.49	13.8	-2.86	0.83
H + h2 -> H2 + H	5.23	10.68	9.6	-5.45	-4.37
OH + NH3 -> H2O + NH2	3.3	7.55	3.2	-4.25	0.1
NH2 + H2O -> NH3 + OH	13.7	17.07	13.2	-3.37	0.5
HCl + CH3 -> Cl + CH4	1.08	3.72	1.8	-2.64	-0.72
CH4 + Cl -> CH3 + HCl	6.09	11.37	7.8	-5.28	-1.71
OH + C2H6 -> H2O + C2H5	4.4	6.46	3.4	-2.06	1
H2O + C2H5 -> OH + C2H6	21.89	21.22	20.7	0.67	1.19
F + H2 -> H + HF	1.83	3.31	1.8	-1.48	0.03
H + HF -> F + H2	32.95	31.95	33.2	1	-0.25
OH + CH3 -> O + CH4	8.26	10.32	7.8	-2.06	0.46
O+CH4 -> OH + CH3	9.37	17.84	13.7	-8.47	-4.33
H + PH3 -> PH2 + H2	0.93	4.09	3.2	-3.16	-2.27
H2 + PH2 -> H + PH3	25.55	27.43	25.5	-1.88	0.05
H + ClH' -> HCl + H	14.47	20.66	18	-6.19	-3.53
OH + H -> H2 + O	7.52	10.94	10.1	-3.42	-2.58
O + H2 -> OH + H	8.31	16.53	13.1	-8.22	-4.79
H + trans-N2H2 -> H2 + N2H	8.24	4.27	5.9	3.97	2.34
H2 + N2H -> H + trans-N2H2	42.03	42.88	41.1	-0.85	0.93
H + H2S -> H2 + HS	1.21	5.09	3.6	-3.88	-2.39
HS + H2 -> H + H2S	17.6	21.15	17.4	-3.55	0.2
O + HCl -> OH + Cl	9.92	14.2	9.8	-4.28	0.12
Cl + OH -> O + HCl	13.81	14.32	9.9	-0.51	3.91
CH4 + NH -> NH2 + CH3	19.29	25.39	8.4	-6.1	10.89
CH3 + NH2 -> NH + CH4	9.4	10.67	22.7	-1.27	-13.3
C2H6 + NH -> NH2 + C2H5	16.99	22.46	8	-5.47	8.99
C2H5 + NH2 -> NH + C2H6	11.4	11	18.4	0.4	-7
C2H6 + NH2 -> C2H5 + NH3	11.56	14.48	10.4	-2.92	1.16
NH3 + C2H5 -> C2H6 + NH2	18.65	19.71	17.8	-1.06	0.85
NH2 + CH4 -> CH3 + NH3	13.5	17.09	14.5	-3.59	-1
NH3 + CH3 -> CH4 + NH2	16.29	19.06	17.9	-2.77	-1.61
$C_5H_8 \rightarrow C_5H_8$	34.76	44.27	38.4	-9.51	-3.64

Table 6: A comparison of HF-DFT activation energies (in kcal/mol) with HF and KS-DFT. The structures are optimized at the HF-DFT level using the MG3 basis set.

Reactions	HF/MG3 // HF/MG3		HFDFT/MG3// HFDFT/MG3		DFT/MG3//DFT/MG3		Best	
	Forward	Back	Forward	Back	Forward	Back	Forward	Back
$CH_3 + H_2$ $H + CH_4$	22.1	23.6	10.8	11.1	7.2	7.8	12.1	15
H CH_3OH $CH_2OH + H_2$	20.1	24.2	5.7	14.7	1.0	11.7	7.3	13.8
$F + H_2$ $H + HF$	-0.1	14.1	2.0	33.2	0.0	32.3	1.8	33.2
$H + PH_3$ $PH_2 + H_2$	11.5	31.4	1.7	26.2	0.0	24.2	3.2	25.5
H + ClH` HCl + H`	31.5	31.5	14.5	14.5	9.8	9.8	18	18
OH + H $H_2 + O$	18	32.9	9.4	10.1	1.6	1.0	10.1	13.1
$H + H_2S$ $H_2 + HS$	12.7	27.8	2.0	18.4	0.0	16.1	3.6	17.4
O + HCl OH + Cl	28.3	20	11.8	15.7	-3.2	2.0	9.8	9.9
$CH_4 + NH$ $NH_2 + CH_3$	39.3	20.5	19.3	9.5	13.6	3.6	22.7	8.4
$C_2H_6 + NH$ $NH_2 + C_2H_5$	37.4	21.1	16.8	11.2	10.1	5.2	18.4	8
$C_2H_6 + NH_2$ $NH_3 + C_2H_5$	30.1	30.7	12.1	19.1	5.2	12.8	10.4	17.8
$NH_2 + CH_4$ $CH_3 + NH_3$	31.9	30	13.7	16.5	7.8	10.4	14.5	17.9

Table 6-1: Error analysis of the activation energies.

Mean Errors	(Method-Best) Kcal/mol	Absolute(Method-Best) Kcal/mol
Hartree-Fock	12.6	12.9
HF-DFT	-1.0	1.6
DFT	-6.6	6.6

Table 6-2: . Error analysis of above 12 reaction's Transition state geometries.

Mean Errors	(QCISD-method) Bond distance in Angstrom	(QCISD-method) Bond angle in degree
Hartree-Fock	0.1	5.2
HF-DFT	0.02	2.6
DFT	0.11	0.5

Enhancing the Capabilities of ACES II

Development and Implementation of the Intrinsic Reaction Coordinate (IRC):

We have implemented the state-of-the-art IRC method into ACESRATE to map the reaction paths. In this module, the IRC is calculated using the quantum mechanical data generated by means of ACES II and ACES III. The commonly used two algorithms have been implemented:

(1) Euler algorithm,
(2) Page-McIver algorithm,

as well as the newly developed correction method on top of those two kinds of IRC paths:

(3) Euler and Page-McIver algorithm with correction.

The Euler method (1) needs only the energy and gradient from quantum chemical calculations in each step and thus, is feasible without heavy quantum chemical calculations. However, to obtain the highly accurate IRC, which is mandatory for the rate constant calculations, a very small step size is required to accurately follow the IRC causing a prohibitively large number of quantum chemical calculations to be necessary. The Page-McIver method (2) improves the accuracy of following the IRC by requiring, in addition, the information from the Hessian. Consequently, the Page-McIver method is able to use a larger step size with maintaining the accuracy of the IRC and to reduce the number of points on which quantum chemical calculations are performed. Although, the calculation of the Hessian itself is time consuming, the Page-McIver method should be preferred since for the variational transition state theory (VTST) rate constant calculations, the calculation of the Hessian is compulsory anyway.

In the course of several application calculations, we have found typical examples in which the Page-McIver method produces an inadequate IRC. Figure 1 shows the modeled potential surface of the dissociation reaction,

$$CH_3POF_2 \rightarrow CH_3 + POF_2, \qquad (1)$$

in which the reactant has a staggered structure while the products favor the eclipsed conformation. IRC is, theoretically, the path which connects the reactants and products smoothly while keeping the correct Hessian structure (all the eigenvalues which correspond to the modes normal to the IRC are positive) as shown by the dashed line in figure 1. The solid line is the path predicted by the Page-McIver method. Along this path, the Hessian does not hold its correct structure, which makes the calculation of the rate constant unfeasible. We have found that this is because the gradient component corresponding to internal rotation is very small relative to the component corresponding to dissociation and Page-McIver method tends to ignore the small component. We have modified the method to correct the direction of the Page-McIver step by partitioning the Hessian and gradient into the IRC direction and its orthogonal counterparts and by applying energy minimization within the orthogonal space to take full account of the small gradient component.

Figure 3 shows the IRC's produced by the Page-McIver method (red line) and by our correction (blue line.) It is obvious that the improvement of IRC by the new correction

method is remarkable when the Page-McIver method is incapable of generating an IRC even with a very small step size (0.005 Å $amu^{-1/2}$.) Figure 4 also shows the effect of step size used for the Page-McIver with correction method. The step size of 0.1 Å $amu^{-1/2}$ is the choice which is commonly accepted for most of the latest IRC algorithms. As shown in figure 2, all the step size tested in this study produce remarkably accurate IRC's up to a step size of 0.5 Å $amu^{-1/2}$, which is extraordinary large. Table I collects the rate constants estimated from the IRC's calculated with the respective step sizes. It shows that all the rate constants agree very well each other regardless of the step size for the respective temperature. Since the larger step size necessitates fewer quantum chemical calculations, it is evident that the new correction method enables the accurate yet efficient calculations of the IRC which is vital for accurate yet convenient rate constant calculations.

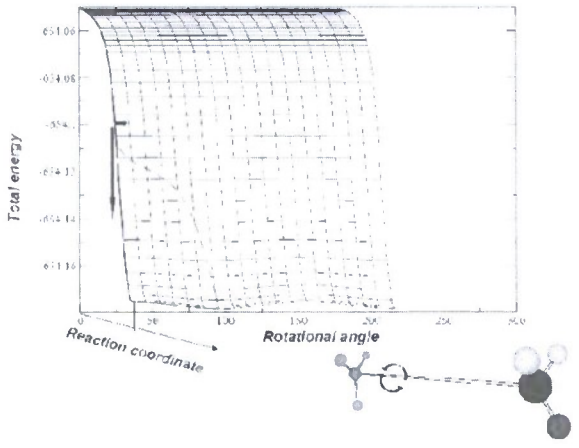

Figure 3. Schematic representation of the potential surface for the reaction (1). The solid line is the IR(calculated with the Page-McIver method while the dashed line is the correct IRC.

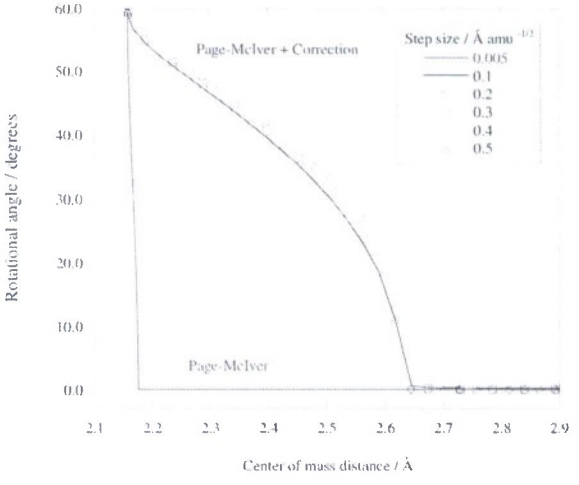

Figure 4. IRC's calculated by means of the Page-McIver method (red) and our correction (blue).

Integration of KS-DFT to ACES II and Implementation of KS-DFT Analytic Gradients:

Not only were the DFT capabilities that were in existence in ACES II underperforming but they also they were not properly integrated to the rest of the ACES II program system. These two limitations were severely hampering the further development of DFT capabilities and implementing gradients, Hessians and higher derivatives on one hand, and on the other, limiting the reactions that could be investigated to small molecules. In order to remedy these limitations we have completed a software integration and improvement of the DFT programs in ACES II system. As a result of these improvements, the current DFT calculations take 2-3 times less than the previous version and can be distributed as part of ACES II. Also, as we have shown in Table 7, that benchmark calculations of B_2H_6 show that ACES II DFT performance is within a factor of three on a per iteration basis, from the NWChem program system. The time taken per iteration is

given in square brackets with the number of iterations in parentheses. It is widely thought that for the standard DFT methods NWChem provides the fastest implementation. As our DFT methods include some that are not standard, HF-DFT and *ab initio dft,* small timings differences will likely be less significant to our objectives.

Table 7: The performance comparison of ACES II and NWChem B_2H_6 KS-DFT implementations (without symmetry; Sun OS).

	Number of functions and memory	ACESII Time (h:m:s)	NWChem
cc-pVDZ	58,15MB	0:2:38 (22) [5]	0:0:24(8) [3]
cc-pVTZ	144,15MB	0:22:25 (23) [58]	0:1:46(8) [13]
aug-cc-pVTZ	230,15MB	1:27:40 (23) [228]	0:10:26(8)[78]
B_2H_6 (with symmetry; Sun OS)			
aug-cc-pVTZ	230,15MB	0:28:34(21) [81]	0:2:34(2) [77]

The analytic gradient capabilities for KS-DFT are also implemented. In Table 8, we show preliminary timing data for ACES II and NWChem KS-DFT single point gradient calculations. Both C_6H_6 and B_2H_6 use D_{2h} symmetry and in both cases, NWChem performs better than ACES II. However, for the N_{10} molecule which uses no symmetry, ACES II outperforms NWChem. While both ACES II and NWChem carry out the numerical integrations only for the symmetry unique atoms, as we can see from the timing data the symmetry processing in the current ACES II KS-DFT gradient implementation needs to be improved to take advantage of the full savings offered by symmetry. This improvement requires computing the gradients in symmetry adapted nuclear center basis. The efforts are currently underway to improve upon the way symmetry being handled in ACES II KS-DFT implementation. However, the determination of rate constants for larger molecules seldom can use symmetry, so for most cases our experience with the unsymmetrical N_{10} would be indicative.

Table 8: A comparison of timing data (in seconds) of ACES II DFT gradients with NWChem (timing data are for the SunOs operating system)

	ACES II	NWChem
C_6H_6 (cc-pVDZ, 114 AOs)	213	45
B_2H_6 (cc-pVTZ, 144 AOs)	213	96
N_{10} (cc-pVDZ, 140 AOs)	862	1011

It is well known that the accuracy of the subsequent rate constants are for the most part dictated by the quality of the electronic structure data. While it is possible to use the state of the art methods such as CCSD(T) with large basis sets to obtain highly accurate data, the cost involved in such a calculation is not practical in some cases. One such case would be when the reactions of interest involve large molecules an example of which would be reactions that are of interest to biochemists. Another such case is when there are many reactions that the rate constants need to be computed for as in the case of an atmospheric decomposition of a pollutant via a multitude of paths. ACES III, which is the newly written, massively parallel version that succeeds ACES II, ameliorates this partly by permitting CCSD(T) and ΛCCSD(T) calculations to be done on thousands of processors.

Other Improvements to the ACES II Program System:

It was observed that as the system size gets bigger (especially for cluster and rings), the geometry optimization with user defined internal or redundant internals becomes impractical: generating user defined internal input is cumbersome when large number of degrees of freedoms are involved and the automatic generation of internals done in the RIC scheme does not have adequate controls to limit the number of internals that it generates. In order to remedy these problems ACES II/III geometry optimization algorithms were enhanced to work with pure Cartesian coordinates (not recommended for small symmetric molecules). Also, an option to specify the connectivities and bypass the automatic generation of internal coordinates to limit the number of internals to the user's requirements is added to the RIC generation algorithm. Another possible solution to the RIC over assignment problem is to prescreen the internal that it automatically assigns and then eliminate the ones that are undesired. Having such an alternative would minimize the user involvement and is being currently implemented.

Development of ACESRATE Program and Rate Constant Calculations

In order to fully utilize the new capabilities being added to ACES II and its parallel version ACES III, we have developed a program capable of computing rate constants with well established methods such as transition state theory (TST) and variational transition state theory (VTST) in house.

$CH+N_2$ Reaction:

The reaction of CH with N_2 is of considerable importance in high temperature combustion chemistry[27]. We have applied ACES II for the electronic state calculations and ACESRATE for the IRC and rate constant calculations of the reaction. We proposed the new reaction mechanism involving the unreported intermediate, HNNC, and investigated the validity of the mechanism by calculating the rate constants and by comparing them to experiment[28]. The reaction consists of following nine elementally reactions:

(1) CH + N2 → INT1 (2) INT1 → INT2 (3) INT2 → INT3
(4) INT1 → INT4 (5) INT4 → INT3 (6) INT2 → HNNC
(7) HNNC → INT4 (8) INT3 → NCN + H (9) HNNC → CNN + H

The reaction mechanism is shown schematically in figure 5. The reactions (1) to (7) are with corresponding transition states and the TST method are used for the rate constant calculation, while for the reactions (8) and (9) which are dissociations without TS's, the VTST rate constants are calculated by searching for the maximum of the free energy (ΔG) potential. The geometric and electronic structures are calculated by means of the CCSD(T) level of theory with the large basis set, aug-cc-pVTZ.

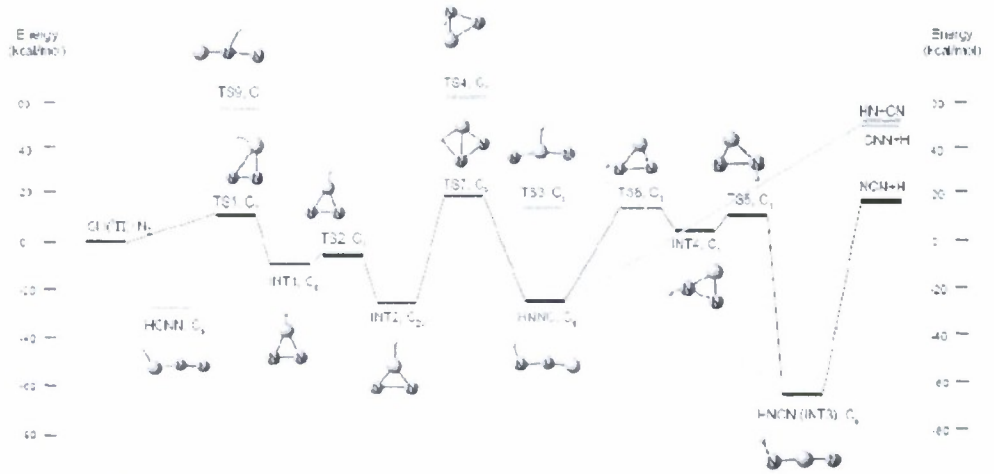

Figure 5. Schematic representation of the reaction mechanism calculated at the CCSD(T)/aug-cc-pVTZ level.

Table 9 shows the calculated rate constants of the respective elemental processes. Within this reaction mechanism, the reaction (8) can be considered to be the rate determining step. Although the agreement with the experimental value is reasonable and better at higher temperatures, the calculated rate constant is still smaller by about an order of magnitude at the highest temperature. However, it is known that more

accurate electron correlation treatments and larger basis sets reduce the barrier height of the reaction, to give a larger rate constant. We will report basis set limit CCSD(T) thermodynamics and kinetics of CH_2+N_2 reaction in a review article dedicated to this reaction[29].

Table 9. Rate constants for the respective elementally reaction calculated by CCSD(T)/aug-cc-pVTZ. The experimental values are also shown.

reaction	k [cm^3 mol^{-1} s^{-1}]				
	2662K	3065K	3352K	3550K	3820K
(1)	5.313E+12	8.455E+12	1.121E+13	1.338E+13	1.668E+13
(2)	1.013E+13	1.142E+13	1.223E+13	1.273E+13	1.337E+13
(3)	1.525E+11	3.881E+11	6.590E+11	9.036E+11	1.319E+12
(4)	2.723E+08	1.617E+09	4.433E+09	8.089E+09	1.662E+10
(5)	1.455E+13	1.725E+13	1.900E+13	2.012E+13	2.156E+13
(6)	1.239E+10	3.974E+10	7.689E+10	1.140E+11	1.826E+11
(7)	1.570E+10	4.397E+10	7.876E+10	1.115E+11	1.689E+11
(8)	8.491E+07	6.674E+08	2.131E+09	4.245E+09	9.653E+09
(9)	4.134E+08	2.580E+09	7.252E+09	1.340E+10	2.791E+10
exptl.	5.63E+10	1.30E+11	1.40E+11	2.00E+11	2.55E+11

Thermal Rate Constants of a Selection of Gas Phase Reactions from the Calibration set Established by Truhlar and Coworkers.

The electronic structure calculations for all 40 reactions in the set are carried out with CCSD(T)/MG3, ΛCCSD(T)/MG3 and HF-DFT/MG3 level to obtain reactants and transition states structures, energies and the vibrational frequencies in order to obtain the corresponding TST and VTST rate constants (the frequencies oat extra points near the transition state are also obtained at the corresponding level). A subset from the entire collection of results is presented here for the discussion purposes and the entire collection will be published elsewhere[31,32].

CCSD(T) and ΛCCSD(T)

In Table 10, we show the TST rate constants obtained at the CCSD(T) level. We also calculate the full Arrhenius plot and compare it with the literature values. Figure 6 shows the Arrhenius plots for three of the hydrogen exchange reactions at the CCSD(T) level. We observe a generally good agreement in the shape of the curve and the values between calculated rate constants and experimental rate constants for the temperature range > 800 K. Also note that when more than one experimental plot is available, the theoretical curves may be used to arbitrate discrepancies between sets of experimental data. Another that at different temperatures, different transition states may be accessed for a particular reaction which is usually indicated by good agreement with the calculated rate constant in one temperature range and poor agreement at a different

temperature range. Therefore imperfect agreement between experiment and calculation may not always be due to the poor quality of the electronic structure calculation

Table 10: Rate constants computed at 700 K. This temperature was chosen as most experimental data in the literature has data points in this temperature range

reactions	Exp. Lit. Value 1	Exp. Lit. Value 2	CCSD(T)/MG3	Absolute Error
Cl + H2 -> HCl + H	1.38E-012	1.79E-012	1.61E-012	2.60E-14
H+HCl --> Cl + H2	2.02E-012	1.40E-012	1.24E-012	4.70E-13
OH + H2 -> H + H2O	6.28E-013	5.66E-013	1.02E-014	5.87E-13
H+H2O -> OH + H2	2.49E-017	4.71E-017	2.96E-017	6.35E-18
F + H2 -> H + HF	7.52E-011		3.71E-010	2.96E-10
H + HF -> F + H2	9.34E-021		2.96E-020	2.03E-20
OH + H -> H2 + O	4.62E-014	1.47E-013	1.08E-014	8.58E-14
O + H2 -> OH + H	3.68E-014	3.42E-014	3.81E-015	3.17E-14

Figure 6 (A, B, C): Temperature dependence of rate constants for three hydrogen exchange reactions selected from Table 3 at the CCSD(T)/MG3 level of optimization and frequency calculations.

A. Cl + H2 → HCl + H

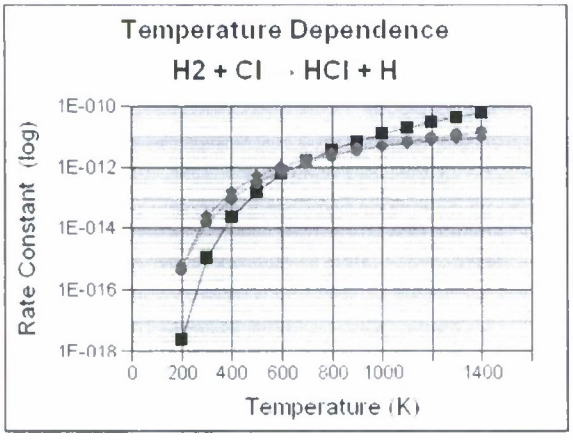

B. H + HF → F + H2

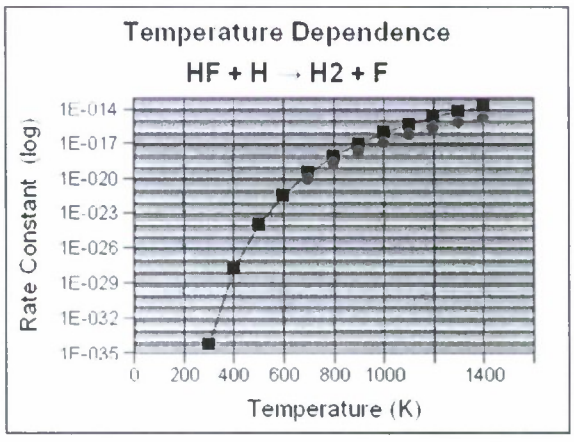

C. OH + H → H2 + O

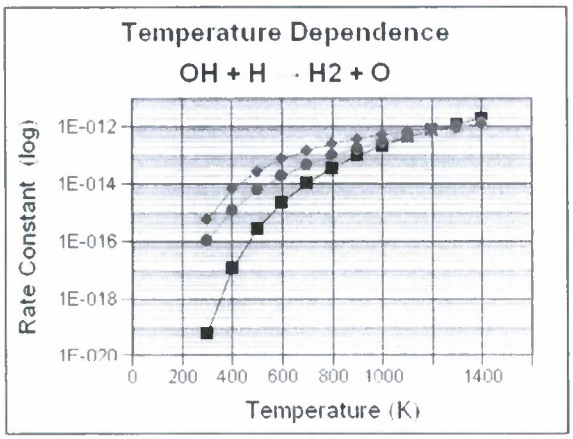

HF-DFT

A selection of HF-DFT TST rate constants computed at 600K are shown in Table 11. For those reactions that are shown in Table 11, the HF-DFT TST rate constants show a remarkable agreement with experiment. For reactions, $F + H_2$ HF, $O + H_2$ $O + H_2$, OH + H $H_2 + O$ we note that the HF-DFT rate constant are in agreement with the CCSD(T) values shown Table 10. Such comparison for all the reactions in the list will be published[31].

Table 11: HF-DFT rate constants.

Reactions	Experimental forward rate constant (cm^3 $molecule^{-1}s^{-1}$) at 600K	HF-DFT forward rate constant (cm^3 $molecule^{-1}s^{-1}$) at 600K
$CH_3 + H_2$ H $+ CH_4$[33]	$1.7*10^{-16}$	$1.35*10^{-16}$
H $+ CH_4$ $CH_3 + H_2$[34]	$2.57x10^{-15}$	$6.26*10^{-15}$
H $+ PH_3$ $H_2 + PH_2$	$6.2*10^{-12}$	$1.15*10^{-11}$
F $+ H_2$ HF + H[34]	$7.39x10^{-11}$	$2.52*10^{-11}$
O $+ H_2$ OH + H[34]	$1.14x10^{-14}$	$4.39*10^{-16}$
OH + H O $+ H_2$[34]	$1.89x10^{-14}$	$1.37*10^{-16}$
O + HCl OH + Cl[34]	$2.62x10^{-14}$	$2.68*10^{-16}$
OH + Cl O + HCl[34]	$8.34x10^{-14}$	$3.00*10^{-17}$

Summary.

New methods including HF-DFT and ΛCCSD(T) have been developed in this STTR, including their analytical gradients. We have also developed a much improved method

for generating accurate IRC's. In addition we have interfaced ACES II and III to our own ACESRATE, also developed for this project, and other packages like POLYRATE to do such rate constant calculations while using the electronic-structure information from ACES. The latter's performance was enhanced while adding analytical gradients for DFT and the previously unexplored HF-DFT, which is the simplest possible correlated method for determining the electronic structure of molecules. This is complimented by ΛCCSD(T) which is the highest level of electronic structure theory that can be expected to be routinely applicable to a large number of systems. Extensive numerical results show the performance of these tools for rate constants and related properties. As ACES II, ACES III, and ACESRATE are freely distributed, these methods can be extensively applied by non-experts to their own problems.

References:

1. **B. J. Finlayson-Pitts and J. N. Pitts, Jr., Chemistry of the Upper and Lower Atmosphere. (Academic Press, San Diego, 2000).**
2. **S. W. Benson, Thermochemical Kinetics, 2nd ed. (Wiley, New York, 1976).**
3. **J. I. Steinfeld, J. S. Francisco, and W. L. Hase, Chemical Kinetics and Dynamics, 2 ed. (Prentice-Hall, 1998).**
4. **J. A. Miller, Faraday Discussions 119, 461 (2001).**
5. **R. Sumathi and W. H. Green, Theoret. Chem. Acc. 108 (4), 187 (2002).**
6. **N. W. Moriarity and M. Frenklach, presented at the Twenty Eighth Symposium (International) on Combustion, University of Edinburgh, Edinburgh, Scotland, 2000 (unpublished).**
7. **R. S. Zhu and M. C. Lin, J. Chem. Phys. 119 (20), 10667 (2003).**
8. **J. F. Stanton, J. Gauss, W. J. Lauderdale, and R. J. Bartlett, Int. J. Quantum Chem. S26, 879 (1992).**
9. **HyperChem, a product of Hypercube, Inc. (1115 NW 4th St., Gainesville, Florida, 32601, 2005).**
10. **Y.-Y. Chuang, J. C. Corchado, P. L. Fast, J. Villà, W.-P. Hu, Y.-P. Liu, G. C. Lynch, K. A. Nguyen, C. F. Jackels, M. Z. Gu, I. Rossi, E. L. Coitiño, S. Clayton, V. S. Melissas, R. Steckler, B. C. Garrett, A. D. Isaacson, and D. G. Truhlar, POLYRATE-version 8.1 (University of Minnesota, Minneapolis, MN, 1999).**
11. **V. Mokrushin and W. Tsang, ChemRate. A Calculational Data Base for Unimolecular Reactions (National Institute of Standards and Technology, Gaithersburg, MD, 2000).**
12. **S. J. Klippenstein, A. F. Wagner, S. H. Robertson, R. Dunbar, and D. M. Wardlaw, VariFlex Software (1999).**
13. **S. C. Smith, E. W.-G. Diau, and H. W. Schranz, UNIRATE, Energy and Angular Momentum Resolved Generalized Transition State Theory Fortran Code (2001).**
14. **J. R. Barker, Int. J. Chem. Kinetics 33 (4), 232 (2001).**
15. **J. R. Barker, N. F. Ortiz, J. M. Preses, and L. L. Lohr, MultiWell-1.4.1 Software (http://aoss.engin.umich.edu/multiwell/, Ann Arbor, Michigan, USA, 2004).**
16. **K. Runge, M. G. Cory, and R. J. Bartlett, J. Chem. Phys. 114, 5141 (2001).**
17. **W. H. Thompson and W. H. Miller, J. Chem. Phys. 106, 142 (1997).**

18. D. Skouteris, D. E. Manopoulos, W. Blan, H.-J. Werner, H.-H. Lai, and K. Liu, Science 286, 1713 (1999).
19. K. Raghavachari, G. W. Trucks, J. A. Pople, and M. Head-Gordon, Chem. Phys. Lett 157, 479 (1989).
20. S. Kucharski and R. J. Bartlett, JCP 108 5243, (1998).
21. A. Taube and R. J. Bartlett, J. Chem. Phys. 128, 044110 (2008).
22. A. Taube and R. J. Bartlett, J. Chem. Phys. 128, 044111 (2008).
23. J. Phys. Chem. A, Vol. 104, No. 21, 2000, Page 4811 and references therein and also see http://comp.chem.umn.edu/database/
24. N. Oliphant and R. J. Bartlett, J. Chem. Phys. 100, 6550 (1994).
25. P. Verma, S. A. Perera and R. J. Bartlett, In preparation.
26. B. G. Lynch and D. G. Truhlar, J. Phys. Chem A,Vol. 105, 2936, 2001.
27. M. R. Berman and M. C. Lin, J. Phys. Chem. 87, 3933 (1983); R. A. Brownsword, L. B. Herbert, I. W. M. Smith and D. W. A. Stewart, J. Chem. Soc., Faraday Trans. 92, 1087 (1996); J. A. Miller and C. T. Bowman, Prog. Energy. Combust. Sci. 15, 287 (1989); D. Lindackers, M. Burmeister and P. Roth, in: 23rd Symp. (Int.) Combust. Proc., pp 251-257 (1990).
28. M. Berman, T. Tsuchiya, A. Gregušová, S. A. Perera and R. J. Bartlett J. Phys. Chem. A. 111 (29), 6894 (2007).
29. A. Gregušová, S. A. Perera, M. Berman and R. J. Bartlett, In Preparation.
30. S.S. Kumaran, K.P.Lim, J.V. Michael, J. Chem. Phys. 101, 9487 – 9498 (1994); T.C. Allison, G.C. Lynch, D.G. Truhlar,and M.S. Gordon, J. Phys. Chem.100, 13575 – 13587 (1996); R.C. Oldenborg, G.W. Loge, D.M. Harradine, and K.R. Winn, J. Phys. Chem.96, 8426 – 8430 (1992); D.L. Baulch, C.J. Cobos, R.A. Cox, C. Esser, P. Frank, T. Just, J.A. Kerr, M.J. Pilling, J. Troe, R.W. Walker, and J. Warnatz, J. Phys. Chem. Ref. Data 21, 411 – 429 (1992); N. Cohen, and K.R. Westberg, J. Phys. Chem. Ref. Data 12 (1983); W. Tsang, and R.F. Hampson, J. Phys. Chem. Ref. Data 15 (1986); M. Yoshimura, M. Koshi, H. Matsui, K. Kamiya, and H. Umeyama, J. Chem. Phys. Lett. 189, 199 – 204 (1992); D.L. Baulch, J. Duxbury, S.J. Grant, and D.C. Montague, J. Phys. Chem. Ref. Data 10 (1981); G.Y.Adusei, and A. Fontijn, Symp. Int. Combust. Proc. 25, 801 – 808 (1994) F. Kaufman,and F.P. Del Greco, Symp. Int. Combust. Proc. 9 (1963); K. Natarajan, and P. Roth, Combust. Flame 70, 267 – 279 (1987).
31. P. Verma, S. A. Perera, A. Gregušová,, A. Melnichuk and R. J. Bartlett, In Preparation.
32. A. Gregušová, S. A. Perera, P. Verma and R. J. Bartlett, In Preparation.
33. B. J. Lynch, P. L. Fast, M. Harris and D. G. Truhlar, J. Chem. Phys. A 104, 4811, (2000).
34. NIST kinetics data base (http://kinetics.nist.gov/kinetics/index.jsp)